CHEMISTRY OF MATERIALS

VOLUME 21, NUMBER 12 JUNE 23, 2009

Communications

The Remarkable and Intriguing Resistance to Oxidation of 2D Ordered hcp Co Nanocrystals. A New Intrinsic Property

Isabelle Lisiecki,[†] Stuart Turner,[‡] Sara Bals,[‡] M. P. Pileni,*[,†] and Gustaaf Van Tendeloo[‡]

Laboratoire LM2N, UMR CNRS 7070, Université P. et M. Curie, bât. F, B.P. 52, 4 place Jussieu, F-75231 Cedex 05, France, and EMAT, University of Antwerp, Groenenborgerlaan 171, 2020 Antwerp, Belgium

Received January 30, 2009
Revised Manuscript Received April 2, 2009

In recent years, the self-assembly of inorganic nanocrystals in 2D superlattices has attracted increasing interest. The collective physical properties are neither those of isolated particles nor those of the bulk phase[1−5] and make them good candidates for further applications. When nanocrystals are ordered in 3D superlattices, special optical, magnetic, mechanic, and crystal growth intrinsic properties have been pointed out.[6,7] To the best of our knowledge, at this point in time nothing is known concerning the chemical properties of nanocrystals ordered in 2D and 3D superlattices compared to isolated nanocrystals. In this communication, we report the first intrinsic property related to the stability against oxidation of Co nanocrystals when they are self-ordered in compact hexagonal networks. This is attributed to the nanocrystal ordering that provides a substantial decrease in the permeability of the alkyl chain layer surrounding the particles. Furthermore, we point out that we are the only group succeeding in obtaining Co_{hcp}/CoO nanocrystals self-ordered in 2D long-range hexagonal networks. Indeed, in all the cases given in the literature, the cobalt core has an fcc structure, whereas in the present case, it is hcp single-crystal.[8−10]

Polycrystalline phases of cobalt nanocrystals stabilized by dodecanoic acid chains are synthesized by chemical reduction in reverse micelles (water in oil droplets) as described in a previous paper.[11] At the end of the synthesis, the native Co nanocrystals, characterized by an average diameter of 7 nm and a size distribution of 9%, are dispersed in hexane. The colloidal solution of native Co nanocrystals is deposited dropwise onto a copper grid coated with amorphous carbon. The sample is then annealed at 350 °C for 20 min under a nitrogen flux and subsequently cooled to room temperature in a nitrogen glovebox. This annealing improves the nanoparticle crystallinity from a poorly crystallized fcc to a monocrystalline hcp structure while maintaining the integrity of the 2D mesoscopic structure.[12] Figure 1a shows a bright-field transmission electron microscopy (TEM) image of a 2D array of Co nanocrystals (7.5 ± 0.4 nm). The main population spontaneously orders regularly in a 2D hexagonal network (zone 1). Some areas, consisting of either disordered

* Corresponding author. E-mail: pileni@sri.jussieu.fr.
[†] Université P. et M. Curie.
[‡] University of Antwerp.

(1) Pileni, M. P. *J. Phys. Chem. B* **2001**, *105*, 3358.
(2) Pileni, M.P. J. *Phys.: Condens. Matter.* **2006**, *18*, S67.
(3) Taleb, A.; Petit, C.; Pileni, M. P. *J. Phys. Chem. B* **1998**, *102*, 2214.
(4) Petit, C.; Taleb, A.; Pileni, M. P. *Adv. Mater.* **1998**, *10*, 259.
(5) Mueggenburg, K. E.; Lin, X. M.; Goldsmith, R. H.; Jaeger, H. M. *Nat. Mater.* **2007**, *6*, 656.
(6) Pileni, M. P. *Acc. Chem. Res.* **2007**, *40*, 685.
(7) Pileni, M. P. *Acc. Chem. Res.* **2008**, *41*, 1799.
(8) Gangopadhyay, S.; Hadipanayis, G. C.; Sorensen, C. M.; Klabunde, K. J. *J. Appl. Phys.* **1993**, *73*, 6964.
(9) Tracy, J. B.; Bawendi, M. G. *Phys. Rev. B* **2006**, *74*, 184434.
(10) Nogués, J.; Skumryev, V.; Sort, J.; Stoyanov, S.; Givord, D. *Phys. Lett.* **2006**, *97*, 157203.
(11) Lisiecki, I.; Pileni, M. P. *Langmuir* **2003**, *19*, 9486.
(12) Lisiecki, I.; Salzemann, C.; Parker, D.; Albouy, P. A.; Pileni, M. P. *J. Phys. Chem. C* **2007**, *111*, 12625.

10.1021/cm900284u CCC: $40.75
Published on Web 05/14/2009

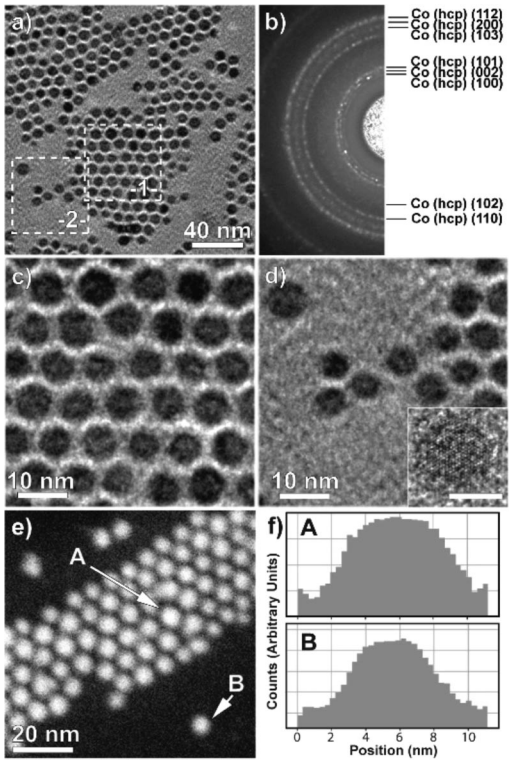

Figure 1. Co nanocrystals before oxidation. (a) TEM image showing hexagonally ordered nanocrystals (zone 1) and disordered or isolated nanocrystals (zone 2). (b) Corresponding electron diffraction pattern showing only Co_{hcp} rings. (c, d) Higher-magnification images of nanocrystals shown in zones 1 and 2 in a. Inset: High-resolution TEM image. The indicated scale bar is 5 nm. (e) HAADF-STEM image of the same sample, the pixel width in the image is 0.32 nm/pixel. (f) Intensity profiles taken over particle A (in the ordered zone) and isolated particle B from e taken using a 5 pixel integration width.

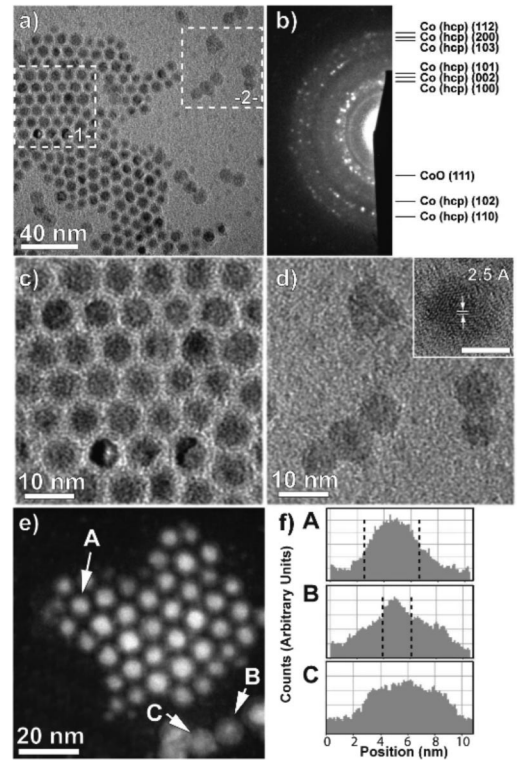

Figure 2. Co nanocrystals after oxidation. (a) TEM image showing hexagonally ordered nanocrystals (zone 1) and disordered or isolated less-contrasted nanocrystals. (b) Corresponding electron diffraction pattern. (c) Higher-magnification image of nanocrystals shown in zone 1. (d) Higher-magnification image of nanocrystals from zone 2 showing structures with a smaller core and/or with absence of contrast. Inset: High-resolution TEM image of an oxidized polycrystalline CoO nanocrystal. The indicated scale bar is 5 nm. (e) HAADF-STEM image of the same sample, the pixel width in the image is 0.12 nm/pixel. (f) Intensity profiles taken over nanocrystal A (in the ordered zone) and nanocrystals B and C from the disordered zone in e using a 5 pixel integration width. Nanocrystal C has a noncontrasted structure showing no steplike features. The core−shell structure is visible for A and B from the intensity step in the profile. The core−shell boundary is indicated by the dashed lines.

or isolated nanocrystals (zone 2) are in coexistence with the ordered arrays. These areas form because of the roughness of the amorphous carbon that hinders the diffusion of these nanocrystals during the solvent evaporation.[13] The mean particle size remains unchanged in the various zones, and no coalescence is observed (images c and d in Figure 1). In the 2D superlattices, the nanocrystal contours are well-defined and the absence of a core−shell contrast suggests a lack of oxidation.

Indeed, the electron diffraction (ED) pattern (Figure 1b) obtained from areas that contain both ordered and disordered crystals shows only sharp rings corresponding to the hcp structure of the highly crystalline Co nanoparticles, and no evidence for the presence of CoO or Co_3O_4 is found. The high crystallinity of the particles also appears through the high-resolution TEM (HRTEM) image (inset in Figure 1d) showing a single-crystal with three lattice planes corresponding to the hcp structure in the [001] zone axis orientation. The absence of a core−shell structure is further confirmed using high-angle annular dark-field scanning transmission electron microscopy (HAADF-STEM). The contrast in this type of image scales with the thickness of the sample and the atomic number *Z*. In Figure 1e, a HAADF-STEM image of the coexisting ordered and isolated system is presented. The line profiles taken across nanocrystal A (in an ordered area) and isolated nanocrystal B noted in Figure 1e are regular without any steplike intensity characteristic of a core−shell boundary. To investigate the resistance to oxidation of the Co nanocrystals, we exposed the sample to air for some hours. The structural changes occurring during this step are shown in Figure 2. From the TEM image (Figure 2a) it is clear that the oxidation of the nanocrystals depends strongly on their degree of ordering: (i) In the ordered array (zone 1, which is shown in more detail in Figure 2c), the particles show high contrast. The contours of the cores of the nanocrystals remain well-defined, but the size has decreased from 7.5 nm to ∼5 nm. In addition, the cores are now surrounded by diffuse intensity (thickness is ∼2 nm), which suggests the presence of a shell-like structure. No coalescence has taken place and the nanocrystals remain regularly ordered in compact hexagonal network. (ii) The disordered area (zone 2) (Figure 2d) shows particles with poorly defined shapes and a poor contrast resulting from a coalescence process. Only a few nanocrystals still reveal a core−shell structure with a reduced core diameter compared to the nanocrystals in the ordered area. The electron diffraction pattern corresponding to the TEM image in Figure 2a (Figure 2b) shows both the signature of hcp Co and cubic CoO. The strongest evidence for the presence of CoO is the

(13) Lisiecki, I.; Albouy, P. A.; Pileni, M. P. *Adv. Mater.* **2003**, *15*, 712.

ring at 2.46 Å, indicative of the (111) lattice spacing. These results are in agreement with those described in ref 14, where Co/CoO core/shell structures were obtained under the same conditions. The inset in Figure 2d shows the HRTEM image of a poorly contrasted particle in the disordered area. Some lattice planes can be observed, and the particle appears to be mostly polycrystalline with a lattice distance of approximately 2.50 Å attributed to CoO. From these results, it is concluded that the nanocrystals located in the ordered array partially oxidize to form core−shell structure Co_{hcp}/CoO, whereas the majority of the population in the disordered area tends to fully oxidize into pure CoO polycrystals. The difference in oxidation behavior between Co nanocrystals with varying degrees of ordering is confirmed using HAADF-STEM (Figure 2e). In the ordered arrays, nanocrystals are characterized by a less intense shell than the core. This is in good agreement with an outer oxide shell, being less dense along the beam direction in comparison to the Co core. The varying oxidation behavior of nanocrystals in different positions of the TEM grid (Figure 2e) can be compared by means of intensity line profiles (Figure 2f): (i) The line profile of nanocrystal A located in the ordered array shows a core of ∼4.5 nm diameter with a high intensity and a ∼2 nm thin shell with a lower intensity. In contrast to the pure hcp Co nanocrystal (Figure 1f), the core−shell boundary can be seen through a step in the intensity profile indicated by the dashed lines. (ii) For isolated nanocrystals, the contrast differs from one nanoparticle to another (Figure 2e). Let us consider two profiles corresponding to nanoparticles B and C showing different contrast profiles. Compared to nanocrystal A, nanocrystal B has a smaller core of ∼2 nm, and a thicker shell of ∼3 nm. The profile for nanocrystal C shows no intensity steps and has a lower intensity, indicating that it is a fully oxidized nanocrystal. Using TEM and HAADF-STEM measurements, we have obtained a total average particle diameter ∼8−9 nm, which is larger than the 7.5 nm observed for nonoxidized Co hcp nanocrystals. This difference is attributed to the lower density of the CoO material compared to the hcp metallic Co. From these results, we have clearly demonstrated that self-assemblies of Co nanocrystals that undergo an oxidation process form core−shell (Co/CoO) nanocrystals assemblies.

This proves that the oxidation process is hampered when nanocrystals are ordered in a hexagonal network, whereas the oxidation process tends to be complete for disordered or isolated nanocrystals. To produce further evidence of the remarkable resistance to oxidation of regularly ordered Co nanocrystals, we employed elemental mapping techniques (energy-filtered TEM (EFTEM)). Chemical maps are obtained by using only electrons with an element-characteristic energy loss to form the image. The zero-loss map shown in Figure 3a is taken as a reference and can be regarded as a filtered bright-field TEM image. The color map (Figure 3b), resulting from the maps obtained using the Co−M edge at 62 eV energy loss and the O−K edge at 532 eV energy loss, respectively, reveals a Co signal (in red) that mainly originates from the core region. Obviously, the Co signal is most pronounced in the cores of the particles and shows lower intensity in the shells. The oxygen signal (in blue) is seen to originate mainly from the shell region, but also from the space between the core−shell structures in the ordered array and from the poorly contrasted isolated nanocrystals. To a lesser extent, it is also found in the uncovered carbon film. The O signal, originating from the shells, reveals the presence of the oxide CoO. The remaining O background is attributed to oxygen molecules still trapped in the alkyl chain of the dodecanoic acid molecules and in the carbon film. The elemental mapping technique gives clear evidence of the presence of large Co core regions in the ordered array, with sizes tending to decrease toward the edges of the array and the surrounding isolated nanocrystals. The Co material is partially or fully transformed into CoO oxide, as has been shown by the other techniques.

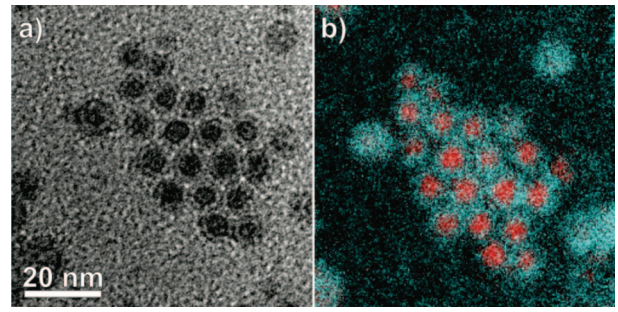

Figure 3. EFTEM maps of Co nanocrystals after oxidation showing: (a) zero-loss map, (b) color map. The cobalt signal is imaged in red and the oxygen signal in blue.

This study permits us to conclude that Co nanocrystals closely packed in a 2D hexagonal network are more robust against oxidation than those isolated or in a disordered area. To explain such behavior, we propose that this enhanced stability is due to a decrease in the permeability of the dodecanoic acid chains to oxygen molecules. The dry oxidation of metallic material occurs in three steps that initiate with the adsorption of oxygen molecules at the metallic surface, followed by the germination and growth steps of the oxide. The adsorption of oxygen at the metallic surface assumes that these molecules may permeate into the layer of the alkyl chains and approach the nanocrystal surface. The isolated or disordered nanocrystals are surrounded by a single layer of alkyl chains that provides a substantial barrier for oxygen molecules. Note that because of the heat treatment, the chains could have undergone a degradation to finally form a shell of lying chains on the nanocrystal surface. However, as most of these nanocrystals can be dissolved again after their annealing, only a partial degradation takes place. In the 2D arrays, the alkyl chains are confined to the nanocrystal surfaces and to the spaces between the nanocrystals because of either their interdigitation from neighboring nanocrystals or the formation of the shells.[11,13,15] These densely packed alkyl chains are consequently much more resistant to oxygen penetration compared to the single-layer configuration. Therefore, the alkyl

(14) Lisiecki, I.; Walls, M.; Parker, D.; Pileni, M. P. *Langmuir* **2008**, *24*, 4295.
(15) Pradeep, T.; Mitra, S.; Nair, A. S.; Mukhopadhyay, R. *J. Phys. Chem. B* **2004**, *108*, 7012.
(16) Ishibashi, M.; Itoh, M.; Nishiraha, H.; Aramaki, K. *Electrochim. Acta* **1996**, *41*, 241.
(17) Mueggenburg, K. E.; Lin, X.-M.; Goldsmith, R. H.; Jaeger, H. M. *Nat. Mater.* **2007**, *6*, 656.

chains do not act merely as mechanical spacers counteracting the core-to-core attraction but also provide an efficient protection against oxidation of the ordered array. Our result is consistent with the work of Ishibashi et al., who found that the permeability of alkaline thiol self-assembled monolayers to oxygen significantly depends on the packing density of the chains. They found that an increase in the chain ordering promoted by an increase in the length of the chains induces a decrease in the permeability to oxygen.[16] Our results are also comparable to the high tensile strength found for 2D superlattices of dodecanethiol-ligated 6 nm diameter gold nanocrystals.[17] Their large effective Young's modulus, on the order of several GPa, appears to be due to the ligand molecules that interact strongly when confined to the interspacing between nanoparticles. The alkyl chains in their confined configuration are responsible for the stable organization of native Co nanocrystals in 2D over few days.[18] After annealing at 350 °C, we have found that these 2D organizations do not coalesce and this strongly implies that the organic chains are still present and that to a certain extent they still protect the nanocrystals. However, the relatively fast oxidation of the nanocrystals after annealing and exposure to air (a few hours compared to few days for the native nanocrystals) indicates that the coating is partially damaged.

To conclude, our results clearly show the remarkable resistance to oxidation of highly crystallized hcp Co nanocrystals close packed in 2D compared to the same nanocrystals either disordered or isolated on the substrate. From a magnetic point of view, these core–shell structures with a high crystalized hcp core are expected to lead to a significant change in the exchange compared to the fcc systems. This intriguing behavior of Co nanocrystals that is related to the permeability of the coating chains to O_2 constitutes the first intrinsic property due to their 2D organization.

Acknowledgment. The authors acknowledge IAP-VI, a project of the Belgian Government, and from the European Union under the Framework 6 program under a contract from an Integrated Infrastructure Initiative (Reference 026019 ESTEEM).

Supporting Information Available: Experimental details (PDF). This material is available free of charge via the Internet at http://pubs.acs.org.

CM900284U

(18) Lisiecki, I.; Parker, D.; Salzemann, C.; Pileni, M. P. *Chem. Mater.* **2007**, *19*, 4030.